Kazanskyite, Ba□TiNbNa3Ti(Si2O7)2O2(OH)2(H2O)4, a Group-III Ti-disilicate mineral from the Khibiny alkaline massif, Kola Peninsula, Russia: description and crystal structure

Revision R1

Kazanskyite, $Ba\square TiNbNa_3Ti(Si_2O_7)_2O_2(OH)_2(H_2O)_4$, a Group-III Ti-disilicate mineral from the Khibiny alkaline massif, Kola Peninsula, Russia: description and crystal structure

F. Cámara[1,*], E. Sokolova[2,3] and F.C. Hawthorne[2]

[1] Dipartimento di Scienze della Terra, Università degli Studi di Torino, via Valperga Caluso 35, 10125 Torino, Italy

[2] Department of Geological Sciences, University of Manitoba, Winnipeg, Manitoba R3T 2N2, Canada

[3] Institute of Geology of Ore Deposits, Petrography, Mineralogy and Geochemistry, Moscow, 119017, Russia

* Corresponding author, E-mail address: fernando.camaraartigas@unito.it

Abstract

Kazanskyite, $Ba\square TiNbNa_3Ti(Si_2O_7)_2O_2(OH)_2(H_2O)_4$, is a Group-III TS-block mineral from the Kirovskii mine, Mount Kukisvumchorr, Khibiny alkaline massif, Kola Peninsula, Russia. The mineral occurs as flexible and commonly bent flakes 2-15 μm thick and up to 330 μm across. It is colourless to pale tan, with a colourless streak and a vitreous lustre. The mineral formed in a pegmatite as a result of hydrothermal activity. Associated minerals are natrolite, barytolamprophyllite, nechelyustovite, hydroxylapatite, belovite-(La), belovite-(Ce), gaidonnayite, nenadkevichite, epididymite, apophyllite-(KF) and sphalerite. Kazanskyite has perfect cleavage on {001}, splintery fracture and a Mohs hardness of 3. Its calculated density is 2.930 g/cm^3. Kazanskyite is biaxial positive with α 1.695, β 1.703, γ 1.733 (λ 590 nm), $2V_{meas.}$ = 64.8(7)°, $2V_{calc.}$ = 55.4°, with no discernible dispersion. It is nonpleochroic. Kazanskyite is triclinic, space group $P\bar{1}$, *a* 5.4260(9), *b* 7.135(1), *c* 25.514(4) Å, *α* 90.172(4), *β* 90.916(4), *γ* 89.964(3)°, *V* 977.61(3) Å^3. The strongest lines in the X-ray powder-diffraction pattern [*d*(Å)(I)(*hkl*)] are: 2.813(100)($12\bar{4}$,$1\bar{2}\bar{2}$), 2.149(82)($22\bar{2}$,$2\bar{2}0$,207,220,$2\bar{2}2$), 3.938(70)($1\bar{1}3$,112), 4.288(44)($11\bar{1}$,$1\bar{1}0$,110,$1\bar{1}1$), 2.128(44)($22\bar{3}$,$2\bar{2}\bar{1}$,$1\bar{3}4$,221,$2\bar{2}3$), 3.127(39)($1\bar{1}6$,115), 3.690(36)($1\bar{1}4$), 2.895(33)($1\bar{2}3$,121) and 2.955(32)($1\bar{2}0$,120,$1\bar{2}2$). Chemical analysis by electron microprobe gave Nb_2O_5 9.70, TiO_2 19.41, SiO_2 28.21, Al_2O_3 0.13, FeO 0.28, MnO 4.65, BaO 12.50, SrO 3.41, CaO 0.89, K_2O 1.12, Na_2O 9.15, H_2O 9.87, F 1.29, O = F -0.54, sum 100.07 wt.%, H_2O was determined from structure refinement. The empirical formula is $(Na_{2.55}Mn_{0.31}Ca_{0.11}Fe^{2+}_{0.03})_{\Sigma3}(Ba_{0.70}Sr_{0.28}K_{0.21}Ca_{0.03})_{\Sigma1.22}(Ti_{2.09}Nb_{0.63}Mn_{0.26}Al_{0.02})_{\Sigma3}Si_{4.05}O_{21.42}H_{9.45}F_{0.59}$, calculated on 22 (O + F) a.p.f.u., *Z* = 2. The structural formula of the form $A^P{}_2M^H{}_2M^O{}_4(Si_2O_7)_2X^O{}_4$ $X^P{}_MX^P{}_A(H_2O)_n$ is $(Ba_{0.56}Sr_{0.22}K_{0.15}Ca_{0.03}\square_{0.04})_{\Sigma1}(\square_{0.74}Ba_{0.14}Sr_{0.06}K_{0.06})_{\Sigma1}(Ti_{0.98}Al_{0.02})_{\Sigma1}(Nb_{0.63}Ti_{0.37})_{\Sigma1}$ $(Na_{2.55}Mn_{0.31}Ca_{0.11}Fe^{2+}_{0.03})_{\Sigma3}(Ti_{0.74}Mn_{0.26})_{\Sigma1}(Si_2O_7)_2O_2(OH_{1.41}F_{0.59})_{\Sigma2}(H_2O)(\square_{0.74}H_2O_{0.26})_{\Sigma1}(H_2O)_{2.74}$. Simplified and ideal formulae are as follows: $Ba(\square,Ba)Ti(Nb,Ti)(Na,Mn)_3(Ti,Mn)(Si_2O_7)_2O_2(OH,F)_2(H_2O)_4$ and $Ba\square TiNbNa_3Ti(Si_2O_7)_2O_2(OH)_2(H_2O)_4$. The Raman spectrum of the mineral

contains the following bands: 3462 cm^{-1} (broad) and 3545 and 3628 cm^{-1} (sharp). The crystal structure was solved by direct methods and refined to an R_1 index of 8.09 %. The crystal structure of kazanskyite is a combination of a TS (titanium silicate) block and an **I** (intermediate) block. The TS block consists of HOH sheets (H-heteropolyhedral, O-octahedral). The TS block exhibits linkage and stereochemistry typical for Group III (Ti = 3 a.p.f.u.) of Ti-disilicate minerals. The TS block has two different H sheets where (Si_2O_7) groups link to [5]-coordinated Ti and [6]-coordinated Nb polyhedra, respectively. There are two peripheral sites, $A^P(1,2)$, occupied mainly by Ba (less Sr and K) at 96 and 26%. There are two **I** blocks: the $\mathbf{I}_1$ block is a layer of Ba atoms; the $\mathbf{I}_2$ block consists of H_2O groups and $A^P(2)$ atoms. The TS and **I** blocks are topologically identical to those in the nechelyustovite structure. The mineral is named in honour of Professor Vadim Ivanovich Kazansky (Вадим Иванович Казанский), a prominent Russian ore geologist and an expert in Precambrian metallogeny.

Keywords: kazanskyite, new mineral, Khibiny alkaline massif, Kola Peninsula, Russia, crystal structure, Group III, Ti-disilicate, TS block

Introduction

Kazanskyite, ideally $Ba\square TiNbNa_3Ti(Si_2O_7)_2O_2(OH)_2(H_2O)_4$, is a new representative of the Ti-disilicate minerals with the TS (titanium silicate) block (Sokolova, 2006). In the crystal structure of kazanskyite, the TS block has the stereochemistry and topology of Group III where Ti + Nb = 3 a.p.f.u. (atoms per formula unit). In Group III, the TS block exhibits linkage 1 where the (Si_2O_7) groups of two H sheets link to the *trans* edges of the Ti octahedron of the O sheet**.** Other Group-III minerals are as follows: lamprophyllite, nabalamprophyllite, barytolamprophyllite, epistolite, vuonnemite, bornemanite and nechelyustovite (Table 1). The crystal structure of kazanskyite is a new structure type and does not have any analogues.

The name is in honour of Professor Vadim Ivanovich Kazansky (Вадим Иванович Казанский) (b. 1926, Tashkent, USSR), a prominent Russian ore geologist and an expert in Precambrian metallogeny. It is particularly appropriate to name this mineral from the Kola Peninsula after Professor Kazansky, as he has worked in the Kola Peninsula for the last 40 years, focusing on the rocks of the Kola superdeep borehole and their relation to the deep structure of ore districts. The new mineral species and its name have been approved by the Commission on New Minerals, Nomenclature and Classification of the International Mineralogical Association (IMA 2011-007). The holotype specimen of kazanskyite is deposited at the Fersman Mineralogical Museum, Russian Academy of Sciences, Leninskii Pr. 18/2, 117071 Moscow, Russia, catalogue No. 4103/1.

Occurrence and associated minerals

Kazanskyite was discovered in a sample of nechelyustovite (Cámara and Sokolova, 2009) from the underground Kirovskii mine (+252 m level), Mount Kukisvumchorr, Khibiny alkaline massif, Kola Peninsula, Russia; this sample is in the mineral collection of Adriana and Renato Pagano, Milan, Italy (Collezione Mineralogica, sample 10161). Following Nèmeth *et al*. (2009),

nechelyustovite is found in one hydrothermally altered pegmatite body emplaced in nepheline syenites near their contact with ijolite–urtites. The pegmatite is a branching vein 0.1–0.5 m wide with a symmetrical zoned structure: a natrolite core, a microcline zone and a marginal aegirine-dominated external zone with subordinate amounts of microcline, nepheline, lamprophyllite and eudialyte. Nechelyustovite (and kazanskyite) is confined to the natrolite core where it forms rosettes up to 1–5 cm in diameter composed of extremely fine (0.01–0.1 mm) bounded flakes and lamellae, embedded in a matrix of natrolite or of carbonate-hydroxylapatite. Other associated are barytolamprophyllite, belovite-(La), belovite-(Ce), gaidonnayite, nenadkevichite, epididymite, apophyllite-(KF) and sphalerite.

Physical and optical properties

The main properties of kazanskyite are presented in Table 2, where they are compared to those of Group-III minerals barytolamprophyllite, bornemanite and nechelyustovite. The mineral forms flakes 2-15 μm thick and up to 330 μm across (Fig. 1). Kazanskyite is colourless to very, very pale tan, with a colourless streak and a vitreous lustre. The mineral is transparent in thin flakes which are flexible and commonly bent. They have a perfect {001} cleavage, splintery fracture and Mohs hardness of 3, and are non-fluorescent under 240-400 nm ultraviolet radiation. The density of the mineral could not be measured owing to the very small thickness of the flakes. Its calculated density (using the empirical formula) is 2.930 g/cm^3. The mineral is biaxial positive with α 1.695, β 1.703, γ 1.733 (λ 590 nm), all ± 0.002, 2V(meas.) = 64.8(7)°, 2V(calc.) = 55.4°, with no discernible dispersion. It is nonpleochroic. Optical orientation is given in Table 3. A Gladston-Dale calculation gives a compatibility index of 0.015, which is rated as superior.

The Raman spectra were collected in back-scattered mode with a HORIBA JobinYvon XPLORA spectrometer interfaced with an LabRAM ARAMIS confocal microscope. A magnification of 100x was used with an estimated spot size of 1 μm, a 1200 grating, an excitation radiation of 532 nm, and a laser power between 5 and 12.5 mW. Calibration was

done using the 520.7 cm^{-1} line of a Si metal. In the OH-stretching region, there is a broad asymmetric envelope with a maximum at 3462 cm^{-1} that may be assigned to various stretches of the H_2O group (Fig. 2). This envelope also has two sharp peaks at 3545 and 3628 cm^{-1} that may be assigned to the principal O-H stretch of OH groups. The small peaks between 2800 and 3000 cm^{-1} are due to C-H stretching vibrations from the small amount of glue used to attach the crystal to a glass fibre. In the lower frequency region, there is a strong envelope centered on 886 cm^{-1} with maxima at 822, 862 and 935 cm^{-1} that may be assigned to Si-O stretches, and two sharp bands at 580 and 680 cm^{-1} that may be assigned to various bending motions of the silicate chain. The lower frequency bands below 480 cm^{-1} are due to various coupled motions (phonon modes) of the structure.

Chemical composition

For the chemical analysis, we used a relatively large platy crystal of kazanskyite with dimensions 0.01 x 0.24 x 0.34 μm. The chemical composition of kazanskyite was determined with a Cameca SX-100 electron-microprobe in wavelength-dispersion mode with an accelerating voltage of 15 kV, a specimen current of 10 nA, a beam size of 5 μm and count times on peak and background of 2 and 10 s, respectively. The following standards were used: $Ba_2NaNb_5O_{15}$ (Ba, Nb), $SrTiO_3$ (Sr), titanite (Ti), diopside (Si, Ca), andalusite (Al), fayalite (Fe), spessartine (Mn), forsterite (Mg), orthoclase (K), albite (Na) and F-bearing riebeckite (F). Ta, Zr, Zn, Mg and Cs were sought but not detected. Data were reduced using the PAP procedure of Pouchou and Pichoir (1985). Under an electron beam, kazanskyite is extremely unstable. The total of ~90 wt% was achieved only for the first point measured, this total being in full agreement with the amount of H_2O calculated from structure refinement. For the next four points, the total increased to ~95 wt%, indicating loss of H_2O. Moreover, attempts to analyze this grain again resulted in much lower values for Na_2O, ~5-6 instead of ~9 wt% for points 1-5 from the first

analysis. We conclude that under the electron beam, kazanskyite first loses H_2O, and then Na and K. To calculate the empirical formula of kazanskyite in accord with the structure results, we used Na_2O and K_2O values from point 1. We did not have material sufficient for direct determination of H_2O, but the presence of H_2O was confirmed by Raman spectroscopy (see above). H_2O was calculated from the results of the crystal structure analysis on the basis of OH + F = 2 p.f.u. and H_2O = 4 p.f.u. (per formula unit). The chemical composition of kazanskyite is given in Table 4. The empirical formula (based on 22 O + F atoms p.f.u.) is $(Na_{2.55}Mn_{0.31}Ca_{0.11}Fe^{2+}_{0.03})_{\Sigma 3}(Ba_{0.70}Sr_{0.28}K_{0.21}Ca_{0.03})_{\Sigma 1.22}(Ti_{2.09}Nb_{0.63}Mn_{0.26}Al_{0.02})_{\Sigma 3}Si_{4.05}O_{21.42}$ $H_{9.45}F_{0.59}$, Z = 2. The structural formula of the form $A^P_2M^H_2M^O_4(Si_2O_7)_2X^O_4X^P_MX^P_A(H_2O)_n$ is $(Ba_{0.56}Sr_{0.22}K_{0.15}Ca_{0.03}\square_{0.04})_{\Sigma 1}(\square_{0.74}Ba_{0.14}Sr_{0.06}K_{0.06})_{\Sigma 1}(Ti_{0.98}Al_{0.02})_{\Sigma 1}(Nb_{0.63}Ti_{0.37})_{\Sigma 1}$ $(Na_{2.55}Mn_{0.31}Ca_{0.11}Fe^{2+}_{0.03})_{\Sigma 3}(Ti_{0.74}Mn_{0.26})_{\Sigma 1}(Si_2O_7)_2O_2(OH_{1.41}F_{0.59})_{\Sigma 2}(H_2O)(\square_{0.74}H_2O_{0.26})_{\Sigma 1}(H_2O)_{2.74}$. Simplified and ideal formulae are as follows: $Ba(\square,Ba)Ti(Nb,Ti)(Na,Mn)_3(Ti,Mn)(Si_2O_7)_2O_2(OH,F)_2(H_2O)_4$ and $Ba\square TiNbNa_3Ti(Si_2O_7)_2O_2(OH)_2(H_2O)_4$.

X-ray powder diffraction

The powder-diffraction pattern for kazanskyite was recorded using a Bruker D8 Discover SuperSpeed micro-powder diffractometer with a Hi-Star multi-wire 2D detector at 15 cm from sample and a modified Gandolfi attachment. Table 5 shows the X-ray powder-diffraction data (for Cu*K*α, λ = 1.54178 Å; 50 kV / 60 mA, two 30-min frames merged) together with the refined unit-cell dimensions; the latter are in close agreement with corresponding values determined by single-crystal diffraction (Table 6).

Crystal structure

X-ray data collection and structure refinement

All crystals of kazanskyite that we were able to find were twinned. X-ray diffraction data for the crystal of kazanskyite were collected with a Bruker AXS SMART APEX diffractometer with a CCD detector (Mo$K\alpha$ radiation). The intensities of 13481 reflections with $-6 < h < 6$, $-8 < k < 8$, $-30 < l < 30$ were collected to 50.05° 2θ using 0.1° frame and an integration time of 60 s. The refined unit-cell parameters were obtained from 5118 reflections with $I > 10\sigma I$ (Tables 2, 6), and an empirical absorption correction (SADABS, Sheldrick, 2008) was applied. The crystal structure of kazanskyite was tentatively solved in space group $P\bar{1}$ by direct methods using SIR 2004 (Burla *et al*., 2005), which supplied an incomplete model with 48 atoms and an *R*-value of 20.1 %. Testing the model with PLATON/twinlat (Spek, 2008) indicated that the crystal of kazanskyite used for structure determination has two components related by the twin matrix (-1 0 0, 0 -1 0, 0 1 1). Twinlat was used to obtain an HKLF5 file and with the Bruker SHELXTL Version 5.1 system of programs (Sheldrick, 2008), the structure model was refined to an R_1 value of 8.09%, the twin ratio being 0.525(3):0.475(3). According to Nespolo and Ferraris (2004) kazanskyite shows twining by metric merohedry. Some of the Si-O and M^H-O distances obtained from the refined structure were not realistic, and we constrained these to more realistic values to obtain better interatomic distances at adjacent sites. Those constrained Si-O and M^H-O distances can be easily detected in the corresponding table as they have an estimated standard deviation of 0.001 Å (non-constrained distances have higher estimated standard deviations). Hence, we chose higher symmetry, space group $P\bar{1}$, to characterize the structure of kazanskyite. Site-scattering values were refined for the $M^O(1)$ and $M^H(1,2)$ sites with the scattering curve of Nb, $M^O(2)$ site (scattering curve of Na), $M^O(3,4)$ sites (scattering curve of Ca) and $A^P(1,2)$ sites (scattering curve of Ba). For the $M^O(2)$ site, refinement converged to an integer value and hence it was subsequently fixed at full occupancy. After refinement of cation occupancies for the $M^H(1)$, $M^O(3,4)$ and $A^P(1,2)$ sites, they were adjusted in accord with the chemical analysis and mean bond lengths, and fixed. For kazanskyite, we observed disorder for

the X^{P}_{A} and *W*(1-7) sites, partly occupied by H_2O and separated by short distances (1.95-2.45 Å). We examined the possibility of H_2O order by refining the structure in lower symmetry. Refinement in space group *P*1 converged to R_1 ~ 7 %, but the structure showed H_2O disorder as in the space group $P\bar{1}$. Hence, we chose higher symmetry, space group $P\bar{1}$, to characterize the structure of kazanskyite. Site occupancies for the X^{P}_{A} and *W*(1-7) sites were refined with U_{iso} fixed at 0.05 Å^2 (analogous to U_{iso} of the X^{P}_{M} site fully occupied by H_2O), and then fixed. At the last stages of the refinement, nine peaks with magnitudes from 1.2 to 3.8 *e*/Å^3 were found in the difference-Fourier map, most of these peaks occurring in the vicinity of the A^{P}(1,2) sites. Occupancies for peaks A^{P}(1A-2B) and 1-3 were refined with the scattering curve of Ba and M^{H}(1A,1B) (Nb) with U_{iso} fixed at 0.02 Å^2. Refined occupancies of these subsidiary peaks vary from 2 to 7 %. Scattering curves for neutral atoms were taken from International Tables for Crystallography (Wilson, 1992). Details of data collection and structure refinement are given in Table 6, final atom parameters are given in Table 7, selected interatomic distances in Table 8, refined site-scattering values and assigned populations for selected cation sites are given in Table 9, and bond valences in Table 10. Tables of structure factors and anisotropic displacement parameters for several atoms have been deposited with the Principal Editor of *Mineralogical Magazine* and are available from www.minersoc.org/pages/e_journals/dep_mat.html.

Site-population assignment

Here we divide the cation sites (Table 7) into 3 groups: M^{O} sites of the O sheet, M^{H} and *Si* sites of the H sheet, and peripheral A^{P} sites; site labeling is in accord with Sokolova (2006). Consider first the Ti- and Nb-dominant sites. We assign cations to these sites based on our knowledge from previous work on Ti-disilicate minerals: (1) Ti- and Nb-dominant sites are always fully occupied; (2) Ti-dominant sites in the O sheet can have a significant content of Mn as in nechelyustovite (Cámara and Sokolova, 2009) and sobolevite,

$Na_{12}Ca(NaCaMn)Ti_2(TiMn)(Si_2O_7)_2(PO_4)_4O_3F_3$ (Sokolova *et al.*, 2005). Table 4 shows that the $2M^H$ and $1M^O$ sites are occupied by 2.09 Ti, 0.63 Nb, 0.26 Mn^{2+} and 0.02 Al (78.57 e.p.f.u.), and the aggregate refined scattering at these sites (75.5 e.p.f.u., Table 9) is in close accord with this composition. The refined site-scattering value at the $M^H(2)$ site is significantly higher, 32.2 e.p.f.u., than that at $M^O(1)$ and $M^H(1)$ sites, <21.7> e.p.f.u., indicating that the heavier atoms, particularly Nb^{5+}, must be assigned to the $M^H(2)$ site. In accord with our knowledge (see above), we assign all Mn [r = 0.83 Å, Shannon (1976)] to the $M^O(1)$ site: 0.74 Ti + 0.26 Mn (cf. 0.67 Ti + 0.33 Mn in nechelyustovite). We assign Ti with minor Al to the $M^H(1)$ site which gives a good match between observed and calculated bond-lengths (Table 9).

Consider next the alkali-cation sites in the O sheet, $M^O(2)$–$M^O(4)$. Table 4 gives 2.55 Na + 0.31 Mn + 0.11 Ca + 0.03 Fe^{2+} = 3 a.p.f.u. with a total scattering of 38.78 e.p.f.u. Site scattering for the alkali sites varies from 11 to 14 e.p.f.u. and the total scattering equals 39 e.p.f.u. This tells us that Na is the dominant cation species at all sites. The $M^O(2)$ site has a mean bond-length of 2.45 Å, whereas the $M^O(3,4)$ sites have significantly shorter mean bond-lengths, 2.33 and 2.29 Å, indicating that the larger Na must be assigned to the $M^O(2)$ site, and Na plus smaller cations, Mn, Ca and Fe^{2+}, must be assigned to the $M^O(3,4)$ sites. This suggestion is supported by individual site-scattering values. As the $M^O(3)$ site has a longer mean bond-length, 2.33 Å, and the $M^O(4)$ site has a shorter mean bond-length, 2.29 Å, we assign all Ca (r = 1.0 Å) to the $M^O(3)$ site and more Mn to the $M^O(4)$ site (r = 0.83 Å) (Table 9). The occurrence of both Na and Mn^{2+} at one site is fairly common in Ti-disilicate minerals; it has been previously described for vuonnemite (Ercit *et al.*, 1998), quadruphite, $Na_{14}Ca_2Ti_4(Si_2O_7)_2(PO_4)_4O_4F_2$ (Sokolova and Hawthorne, 2001), polyphite, $Na_{10}(Na_4Ca_2)_2Ti_4(Si_2O_7)_2(PO_4)_6O_4F_4$ (Sokolova *et al*., 2005), bornemanite (Cámara and Sokolova, 2007) and nechelyustovite (Cámara and Sokolova, 2009).

Consider last the peripheral $A^P(1,2)$ sites, with refined site-scattering values of 42.9 and 11.2 e.p.f.u., respectively (Table 9). The cations to be assigned to these sites are Ba, Sr, K and

Ca, with a total scattering 53.83 e.p.f.u. (Table 4). Although the refined site-scattering at the $A^P(2)$ site is low, 11.2 e.p.f.u., we cannot consider it partly occupied only by a low scattering species, i.e., K (19 el.) as 0.21 K a.p.f.u. (available from chemical analysis) corresponds to a scattering of only ~4 e.p.f.u. Thus we distribute Ba, Sr, K and Ca between the $A^P(1)$ and $A^P(2)$ sites in the ratio 4:1 in accord with the refined site-scattering. Therefore at the $A^P(1)$ and $A^P(2)$ sites, Ba and vacancy are dominant species, respectively (Table 9).

Description of the structure

Site nomenclature

As stated above, the cation sites are divided into 3 groups: M^O sites of the O sheet, M^H and *Si* sites of the H sheet, and peripheral A^P sites. Also in accord with Sokolova (2006), we label the X anions: $2X^O_M$ = common vertices of $3M^O$ and M^H polyhedra; $2X^O_A$ = common vertices of $3M^O$ and A^P polyhedra (where A^P-X^O_A < 3 Å); $2X^P$ = X^P_M and X^P_A = apical anions of M^H and A^P cations at the periphery of the TS block.

Cation sites

In the crystal structure of kazanskyite, there is one TS block composed of H_1 O H_2 sheets. We will describe cation sites of the O sheet, H sheets and peripheral A^P sites.

O sheet

There are four cation sites in the O sheet: the Ti-dominant $M^O(1)$ site and the alkali-cation $M^O(2\text{-}4)$ sites (Fig. 3a). The $M^O(1)$ site is occupied by 0.74 Ti and 0.26 Mn, and is coordinated by four O atoms and two monovalent X^O_A anions (see section on *Anion sites* below) with a $\langle M^O(1)\text{–}\varphi\rangle$ distance of 2.00 Å (φ = unspecified anion) (Tables 7, 8, 9). The

$M^O(2)$ site is occupied by Na (Table 9) and is coordinated by six O atoms, with a <$M^O(2)$–O> distance of 2.45 Å. The $M^O(3)$ and $M^O(4)$ sites are occupied ~80% by Na and 20% by M^{2+} (= Mn, Ca and Fe^{2+}) (Table 9); they are coordinated by four O atoms and two X^O_A anions, with <$M^O(3)$–φ> and <$M^O(4)$–φ> distances of 2.33 and 2.29 Å, respectively. For the O sheet, the total of the $4M^O$ cations is $[(Na_{2.55}Mn_{0.31}Ca_{0.11}Fe^{2+}_{0.03})(Ti_{0.74}Mn_{0.26})]_{\Sigma 4}$, with simplified and ideal compositions $(Na,Mn)_3(Ti,Mn)$ and Na_3Ti a.p.f.u., respectively.

H sheets

In the H_1 and H_2 sheets, there are four tetrahedrally coordinated sites occupied by Si with a <Si–O> distance of 1.62 Å (Table 8, Fig. 3b, c). There are two M^H sites that occur in different H sheets of the TS block. In the H_1 sheet (Fig. 3b), the [5]-coordinated $M^H(1)$ site is occupied mainly by Ti (Table 9) and is coordinated by five O atoms, with a <$M^H(1)$–O> distance of 1.93 Å; the very short $M^H(1)$– $X^O_M(1)$ distance of 1.667 Å (Table 8) is in accord with the structure topology of Group-III minerals (Sokolova, 2006, Fig. 31). In the H_2 sheet (Fig. 3c), the [6]-coordinated Nb-dominant $M^H(2)$ site is coordinated by five O atoms and an H_2O group with a <$M^H(2)$–φ> distance of 1.99 Å (Table 8). The H_2O group is the X^P_M anion in the terminology of Sokolova (2006). The shortest $M^H(2)$-$X^O_M(2)$ distance is 1.824 Å and the longest $M^H(2)$-X^P_M distance is 2.240 Å, from the $M^H(2)$ site to an H_2O group. For the H_1 and H_2 sheets, the total of M^H_2 cations is $[(Ti_{0.98}Al_{0.02})(Nb_{0.63}Ti_{0.37})]_{\Sigma 2}$, with simplified and ideal composition Ti(Nb,Ti) and TiNb a.p.f.u., respectively.

Peripheral A^P sites

In kazanskyite, there are two A^P sites. The [10]-coordinated $A^P(1)$ site is occupied by $Ba_{0.56}Sr_{0.22}K_{0.15}Ca_{0.03}\square_{0.04}$ p.f.u. and is coordinated by O atoms, with $<A^P(1)–O> = 2.83$ Å. The [7]-coordinated $A^P(2)$ site is occupied by $\square_{0.74}Ba_{0.14}Sr_{0.06}K_{0.06}$ p.f.u. (Table 9) and is coordinated by six O atoms and one H_2O group [X^P_A anion in the terminology of Sokolova (2006)], with $<A^P(2)–\varphi> = 2.80$ Å. At the $A^P(1)$ and $A^P(2)$ sites, the dominant species are Ba^{2+} and $\square$, respectively, and we write the ideal composition of these sites as Ba a.p.f.u. and $\square$ p.f.u. To summarize, simplified and ideal compositions of two peripheral sites are Ba($\square$,Ba) and Ba$\square$ p.f.u., respectively.

We write the cation part of the ideal structural formula as the sum of (1) the peripheral sites + (2) two H sheets + (3) O sheet: (1) Ba$\square$ + (2) TiNb + (3) Na_3Ti = Ba$\square$TiNbNa_3Ti with a total charge of 18^+.

Anion sites

There are 14 anion sites, O(1-14), occupied by O atoms which form the tetrahedral coordination of the Si atoms (Tables 7, 8, 10). There are two sites, $X^O_M(1,2)$, which are common anions for the M^H polyhedra and three octahedra of the O sheet (Table 5). These anions receive bond valences of 2.19 and 1.86 v.u., respectively, (Table 10) and hence are O atoms (Table 7). There are two $X^O_A(1,2)$ sites that are common anions for three octahedra of the O sheet and occur just below the A^P cation. They receive bond valences of 1.23 and 1.08 v.u., respectively (Table 10), and hence are monovalent anions (Table 7). The chemical analysis gives F 0.59 a.p.f.u. and we need 2 –0.59 = 1.41 OH p.f.u. to fill these two sites (Table 4). Therefore, we assign $OH_{1.41}F_{0.59}$ to the two $X^O_A(1,2)$ sites. Ideally, the two X^O_A sites give $(OH)_2$ p.f.u. There are two X^P anions. The X^P_M is an apical anion for the $M^H(2)$ cation (Tables 8, 9); it receives bond valence of 0.40 v.u. (Table 10) and is an H_2O group. The X^P_A anion site coordinates the $A^P(2)$ site which is occupied by Ba, Sr and K at 26% (Tables 8, 9) and the X^P_A site is occupied by an anion species at 26% (Table 7). The X^P_A anion receives bond valence of 0.09 v.u. (Table 10) and it is an H_2O

group, giving [$\square_{0.74}(H_2O)_{0.26}$] p.f.u. There are H_2O groups at the seven *W*(1-7) sites, that are not bonded to any cation. The *W*(1-7) sites are partly occupied (Table 7) and give $(H_2O)_{2.74}$ p.f.u.

To conclude, we write the anion part of the ideal structural formula as the sum of the anion sites: O_{14} (O atoms of Si_4 tetrahedra) + O_2 [$X^O_M(1,2)$] + $(OH)_2$ [$X^O_A(1,2]$ + $(H_2O)_4$ [(X^P_M + X^P_A + W(1–7)]. We consider an (Si_2O_7) group as a complex oxyanion and write the anion part of the ideal structural formula as $(Si_2O_7)_2O_2(OH)_2(H_2O)_4$ with a total charge of 18^-.

Based on the SREF results and bond-valence calculations, we write the ideal structural formula of kazanskyite as the sum of the cation and anion components: $Ba\square TiNbNa_3Ti(Si_2O_7)_2O_2(OH)_2(H_2O)_4$, sp. gr. $P\bar{1}$, Z = 2. The validity of the ideal formula is supported by the good agreement between the total charges for cations in the ideal and empirical formulae: 5^+ [for $Ba\square Na_3$] $+13^+$ [Ti_2Nb] = 18^+ versus 5.66^+ [($Ba_{0.70}Sr_{0.28}K_{0.21}Ca_{0.03}\square_{0.78}$) + ($Na_{2.55}Mn^{2+}_{0.31}Ca_{0.11}Fe^{2+}_{0.03}$)] + 12.09^+ [($Ti_{2.09}Nb_{0.63}Mn^{2+}_{0.26}Al_{0.02}$)] = 17.75^+.

Structure topology

The TS block

In the Ti-disilicate minerals (Sokolova, 2006), the TS block consists of HOH sheets where H is a heteropolyhedral sheet including (Si_2O_7) groups, and O is a trioctahedral close-packed sheet. In kazanskyite, there is one unique TS block which consists of H_1 O H_2 sheets (Fig. 3). The O sheet comprises M^O(1-4) octahedra (Fig. 3a). There are two distinct H sheets in kazanskyite. In the H_1 sheet, (Si_2O_7) groups and [5]-coordinated Ti-dominant M^H(1) polyhedra share common vertices to form the sheet (Fig. 3b). In the H_2 sheet, (Si_2O_7) groups share common vertices with Nb-dominant M^H(2) octahedra (Fig. 3c). The topology of the two H sheets is identical except for the coordination of the M^H sites. In the H_1 and H_2 sheets, the peripheral A^P sites are occupied by [10]-coordinated Ba and [7]-coordinated (□,Ba), respectively [see discussion of the (**I**) block below]. The H and O sheets link *via* common vertices of M^H, Si and M^O polyhedra to form the TS block which is parallel to (001) (Fig.3d). In kazanskyite, the TS block exhibits linkage 1 and a

stereochemistry typical of Group III (Sokolova, 2006): (Si_2O_7) groups of two H sheets link to the *trans* edges of the Ti octahedron of the O sheet.

*The **I** blocks*

In kazanskyite, the TS blocks alternate with intermediate (**I**) blocks, $\mathbf{I_1}$ and $\mathbf{I_2}$. An **I** block is always intercalated between two TS blocks, and cations of the **I** block form close-packed **I** layers parallel to the TS block, where m = number of those layers (Sokolova, 2006).

A layer of Ba atoms [$A^P(1)$ sites] forms the $\mathbf{I_1}$ block between adjacent TS blocks (Fig. 4a). In the $\mathbf{I_1}$ block, Ba atoms are arranged in a close-packed fashion where each atom is surrounded by six others at approximately equal distances of 5 Å. The composition of the $\mathbf{I}_1$ block is $A^P(1)_2$ or ideally Ba_2 (= Ba a.p.f.u.).

The $\mathbf{I_2}$ block is composed mainly of H_2O groups and two **I** layers (m = 2) of cations (mainly Ba) at the 26% occupied $A^P(2)$ sites (Fig. 4b). The two **I** layers of $A^P(2)$ atoms are parallel to (001) and are related by an inversion centre. There are two types of H_2O groups in the $\mathbf{I_2}$ block, bonded and non-bonded to cations. H_2O groups at the X^P_M and X^P_A sites are ligands of $M^H(2)$ and $A^P(2)$ cations. The X^P_M and X^P_A sites are occupied at 100 and 26%, respectively, giving $(H_2O)_{2.52}$ [= $(H_2O)_{1.26}$ p.f.u., ideally (H_2O) p.f.u.]. H_2O groups at the *W*(1-7) sites (Table 7, Fig. 4b) are not bonded to any cation; they occur in the intermediate space between two TS blocks and give in total $(H_2O)_{5.48}$ [= $(H_2O)_{2.74}$ p.f.u.]. We write the composition of the $\mathbf{I_2}$ block as the sum of two $A^P(2)$ sites, the X^P_M and X^P_A sites, and seven *W* sites: $(\square_{0.74}Ba_{0.14}Sr_{0.06}K_{0.06})_2 + (H_2O)_{2.52} + (H_2O)_{5.48} = (\square_{0.74}Ba_{0.14}Sr_{0.06}K_{0.06})_2(H_2O)_8$ which corresponds to $(\square_{0.74}Ba_{0.14}Sr_{0.06}K_{0.06})(H_2O)_4$ p.f.u., with simplified and ideal compositions of $(\square,Ba)(H_2O)_4$ and $\square(H_2O)_4$ p.f.u., respectively.

Hydrogen bonding

There is extensive cation and anion disorder in the **I₂** block of kazanskyite. The $A^P(2)$ site is 26% occupied mainly by Ba; the X^P_A and $W(1\text{-}7)$ sites are partly, 25-71%, occupied by H_2O (Table 7). There is a short distance of 2.04 Å between the $A^P(2)$ site and the $W(6)$ site, hence the $W(6)$ site can be occupied by H_2O where the $A^P(2)$ site is vacant (and vice versa). Table 11 reports O–O distances less than 3.2 Å between O atoms of H_2O groups that occupy X^P_M, X^P_A and $W(1\text{-}7)$ sites; short (less than 2.5 Å) distances between partly occupied *W* sites are given in brackets. However, inspection of Table 11 gives O–O distances from 2.50 to 3.20 Å and these distances are suitable for hydrogen bonds (Fig. 4b).

The general structure

The crystal structure of kazanskyite (Fig. 5a) consists of TS and **I** blocks alternating along **c**. There are two symmetrically equivalent TS blocks and two distinct **I** blocks, $\mathbf{I}_1$ and $\mathbf{I}_2$, per *c* unit-cell parameter. The $\mathbf{I}_1$ block has two adjacent H_1 sheets, and the $\mathbf{I}_2$ block has two adjacent H_2 sheets.

The ideal structural formula of kazanskyite

Above, we wrote simplified and ideal formulae of kazanskyite based on the occupancies of the cation and anion sites. Here, we write the ideal structural formula of kazanskyite in accord with Sokolova (2006); we use a modified formula of the TS block of Group-III minerals: $A^P_2B^P_2M^H_2M^O_4(Si_2O_7)_2X^O_4\,X^P_MX^P_A$, where A^P and B^P are cations at the peripheral (*P*) sites; M^H and M^O are cations of the H and O sheets; X^O are anions of the O sheet; X^P_M and X^P_A are apical anions of the M^H and A^P cations at the periphery of the TS block. In kazanskyite, $A^P_2 = A^P(1) + A^P(2) = Ba + \square = Ba\square$; $B^P_2 = 0$; $M^H_2 = M^H(2) + M^H(1) = TiNb$; $M^O_4 = Na_3Ti$; $X^O_4 = O_2(OH)_2$; $X^P_M + X^P_A = (H_2O) + \square = (H_2O)$. Hence, we write the ideal composition of the TS block as follows:

$$^{A^P}[Ba\square]\ ^{M^H}[TiNb]\ ^{M^O}[Na_3Ti](Si_2O_7)_2\ ^{X^O}[O_2(OH)_2]\ ^{X^P_M}[H_2O]\ ^{X^P_A}[\square] =$$

$Ba\square TiNbNa_3Ti(Si_2O_7)_2O_2(OH)_2(H_2O)$, $Z = 2$.

There are two **I** blocks in kazanskyite. The $\mathbf{I}_1$ block comprises the $A^P(1)$ atoms, which have been already counted in the formula of the TS block. The $\mathbf{I}_2$ block includes the $A^P(2)$ atoms and the $X^P_M + X^P_A$ anions, which have been already counted in the formula of the TS block; and (H_2O) groups at the *W*(1-7) sites, ideally $(H_2O)_3$ p.f.u.

We sum the TS block and an H_2O component [W(1-7)] of the $\mathbf{I}_2$ block to write the ideal structural formula for kazanskyite: $Ba\square TiNbNa_3Ti(Si_2O_7)_2O_2(OH)_2(H_2O)_4$, with $Z = 2$.

Related minerals

Kazanskyite is the fourth Ti-disilicate mineral [after bornemanite (Cámara and Sokolova, 2007), cámaraite, ideally $Ba_3NaTi_4(Fe^{2+},Mn)_8(Si_2O_7)_4O_4(OH,F)_7$ (Cámara *et al*., 2009) and nechelyustovite (Cámara and Sokolova, 2009)] and the third Group-III mineral (after bornemanite and nechelyustovite) with two different types of **I** block. Kazanskyite is closely related to nechelyustovite (Fig. 5b). Both minerals contain two **I** blocks of the same topology and composition (Figs. 5a, b): an $\mathbf{I}_1$ block which is a distorted layer of Ba atoms and an $\mathbf{I}_2$ block which contains H_2O groups and A^P sites which are ~25% occupied by Ba. The chemical compositions of both M^H and A^P sites of the **I** blocks are identical in kazanskyite and nechelyustovite. An **I** block which is a distorted layer of Ba atoms occurs also in bornemanite. Nevertheless, nechelyustovite has two different TS-blocks (TS_1 and TS_2; Fig. 5b) while only one is present in kazanskyite and bornemanite. In addition, in nechelyustovite two TS_2-blocks link directly without an intermediate block like TS-blocks link in epistolite (Sokolova and Hawthorne, 2004).

Acknowledgements

We thank Luca Bindi and one anonymous reviewer, Associate Editor Giancarlo Della Ventura and Joint Principal Editor Peter Williams for useful comments. We are very grateful to Renato

and Adriana Pagano, Milan, Italy, who provided a sample of nechelyustovite from their mineral collection (Collezione Mineralogica, sample #10161), in which sample kazanskyite was discovered. FCH was supported by a Canada Research Chair in Crystallography and Mineralogy, by Discovery and Major Installation grants from the Natural Sciences and Engineering Research Council of Canada, and by Innovation Grants from the Canada Foundation for Innovation.

References

Anthony, J.W., Bideaux, R.A., Bladh, K.W. and Nichols, M.C. (1995) *Handbook of Mineralogy. Silica, Silicates.* Mineral Data Publishing, Tucson, Arizona, **2**(1), 46, 355.

Brown, I.D. (1981) The bond-valence method: an empirical approach to chemical structure and bonding. Pp. 1-30 in: *Structure and Bonding in Crystals II* (M. O'Keeffe and A. Navrotsky, editors). Academic Press, New York.

Burla, M.C., Caliandro, R., Camalli, M., Carrozzini, B., Cascarano, G.L., De Caro, L., Giacovazzo, C., Polidoria, G. and Spagna, R. (2005) SIR2004: an improved tool for crystal structure determination and refinement. *Journal of Applied Crystallography*, **38**, 381-388.

Cámara, F. and Sokolova, E. (2007) From structure topology to chemical composition. VI. Titanium silicates: the crystal structure and crystal chemistry of bornemanite, a group-III Ti-disilicate mineral. *Mineralogical Magazine*, **71**, 593-610.

Cámara, F. and Sokolova, E. (2009) From structure topology to chemical composition. X. Titanium silicates: the crystal structure and crystal chemistry of nechelyustovite, a group III Ti-disilicate mineral. *Mineralogical Magazine*, **73**, 887-897.

Cámara, F., Sokolova, E. and Nieto, F. (2009) Cámaraite, $Ba_3NaTi_4(Fe^{2+},Mn)_8(Si_2O_7)_4O_4(OH,F)_7$. II. The crystal structure and crystal chemistry of a new group-II Ti-disilicate mineral. *Mineralogical Magazine*, **73**, 855-870.

Dudkin, O.B. (1959) On barium lamprophyllite. *Zapiski Vsesoyuznogo Mineralogicheskogo Obshchestva*, **88**(6), 713-715 (in Russian).

Ercit, T.S., Cooper, M.A. and Hawthorne, F.C. (1998) The crystal structure of vuonnemite, $Na_{11}Ti^{4+}Nb_2(Si_2O_7)_2(PO_4)_2O_3(F,OH)$, a phosphate-bearing sorosilicate of the lomonosovite group. *Canadian Mineralogist*, **36**, 1311-1320.

454 Ferraris, G., Belluso, E., Gula, A., Soboleva, S.V., Ageeva, O.A. and Borutskii, B.E. (2001) A
455 structural model of the layer titanosilicate bornemanite based on siedozerite and
456 lomonosovite modules. *Canadian Mineralogist*, **39**, 1665-1673.
457 Krivovichev, S.V., Armbruster, T., Yakovenchuk, V.N., Pakhomovsky, Ya. A. and Men'shikov,
458 Yu. P. (2003) Crystal structures of lamprophyllite-2*M* and lamprophyllite-2*O* from the
459 Lovozero alkaline massif, Kola peninsula, Russia. *European Journal of Mineralogy*, **15**,
460 711-718.
461 Men'shikov, Yu.P., Bussen, I.V., Goiko, E.A., Zabavnikova, N.I., Mer'kov, A.N. and Khomyakov,
462 A.P. (1975) Bornemanite - a new silicophosphate of sodium, titanium, niobium and
463 barium. *Zapiski Vsesoyuznogo Mineralogicheskogo Obshchestva*, **104**(3), 322-326 (in
464 Russian).
465 Nèmeth, P., Khomyakov, A.P., Ferraris, G. and Menshikov, Yu.P. (2009) Nechelyustovite, a
466 new heterophyllosilicate mineral, and new data on bykovaite: a comparative TEM study.
467 *European Journal of Mineralogy*, **21**, 251-260.
468 Nespolo, M. and Ferraris, G. (2004) Applied geminography - Symmetry analysis of twinned
469 crystals and definition of twinning by reticular polyholohedry. *Acta Crystallographica*,
470 **A60**, 89-95.
471 Pouchou, J.L. and Pichoir, F. (1985) 'PAP' φ(ρZ) procedure for improved quantitative
472 microanalysis. Pp. 104-106 in: *Microbeam Analysis* (J.T. Armstrong, editor). San
473 Francisco Press, San Francisco, California, USA.
474 Rastsvetaeva, R.K. and Chukanov, N.V. (1999) Crystal structure of a new high-barium analogue
475 of lamprophyllite with a primitive unit cell. *Doklady Chemistry*, **368**(4-6), 228-231.
476 Shannon, R.D. (1976) Revised effective ionic radii and systematic studies of interatomic
477 distances in halides and chalcogenides. *Acta Crystallographica*, **A32**, 751-767.
478 Sheldrick, G.M. (2008) A short history of SHELX. *Acta Crystallographica*, **A64**, 112-122.

Sokolova, E. (2006) From structure topology to chemical composition. I. Structural hierarchy and stereochemistry in titanium disilicate minerals. *Canadian Mineralogist,* **44,** 1273-1330**.**

Sokolova, E. and Cámara, F. (2008) From structure topology to chemical composition. III. Titanium silicates: crystal chemistry of barytolamprophyllite. *Canadian Mineralogist*, **46**, 403-412.

Sokolova, E. and Hawthorne, F.C. (2001) The crystal chemistry of the $[M_3O_{11-14}]$ trimeric structures: from hyperagpaitic complexes to saline lakes. *Canadian Mineralogist*, **39**, 1275-1294.

Sokolova, E. and Hawthorne, F.C. (2004) The crystal chemistry of epistolite*. Canadian Mineralogist*, **42**, 797-806.

Sokolova, E. and Hawthorne, F.C. (2008) From structure topology to chemical composition. IV. Titanium silicates: the orthorhombic polytype of nabalamprophyllite from Lovozero massif, Kola Peninsula, Russia. *Canadian Mineralogist*, **46**, 1469-1477.

Sokolova, E., Hawthorne, F.C. and Khomyakov, A.P. (2005) Polyphite and sobolevite: revision of their crystal structures. *Canadian Mineralogist*, **43**, 1527-1544.

Sokolova, E., Cámara, F. and Hawthorne, F.C. (2011) From structure topology to chemical composition. XI. Titanium silicates: crystal structures of innelite-1*T* and innelite-2*M* from Inagli massif, Yakutia, Russia, and the crystal chemistry of innelite. *Mineralogical Magazine*, **75**, 2495-2518.

Spek, A.L. (2008) PLATON, A Multipurpose Crystallographic Tool, Utrecht University, Utrecht, The Netherlands.

Wilson, A.J.C. (editor) (1992) International Tables for Crystallography. Volume C: Mathematical, physical and chemical tables. Kluwer Academic Publishers, Dordrecht, The Netherlands.

Figure captions

Fig. 1. The crystal of kazanskyite used for measuring optics (~0.015 x 0.090 x 0.175 mm) on a glass fibre in oil, note the platy nature (a) and irregular surface of the crystal (b).

Fig. 2. Raman spectra of kazanskyite in the fingerprint region (a) and the O-H stretching region (b), obtained with 532 nm laser excitation.

Fig. 3. The details of the TS block in the crystal structure of kazanskyite: the close-packed octahedral (O) sheet (a); the heteropolyhedral (H) sheets H_1 (b) and H_2 (c); the TS block (d) viewed down [100]; (SiO_4) tetrahedra are orange, Ti^{4+}- and Nb^{5+}-dominant polyhedra are yellow, Na-dominant octahedra are blue, atoms at the A^P sites are shown as raspberry spheres which are labeled 1 and 2 and correspond to $A^P(1)$ and $A^P(2)$ atoms; monovalent X^O_A anions and H_2O groups are shown as small and large red spheres; in (a), labels 1-4 correspond to $M^O(1\text{-}4)$, respectively; in (b) and (c), labels 1-4 (on orange) correspond to Si(1-4) tetrahedra, respectively, and labels 1 and 2 (on yellow) correspond to $M^H(1)$ and $M^H(2)$ polyhedra, respectively.

Fig. 4. Details of linkage of TS blocks in the crystal structure of kazanskyite: the intermediate (**I**) blocks $\mathbf{I}_1$ (a) and $\mathbf{I}_2$ (b). Legend as in Fig. 3, m = number of cation layers in the **I** block, solid black lines show the positions of the m layers; bonds from the $A^P(2)$ atom to coordinating anions are shown as black lines; in (b), H_2O groups coordinating $M^H(2)$ and $A^P(2)$ atoms are labeled X^P_M and X^P_A, respectively, and H_2O groups at the *W*(1)-*W*(7) sites which do not coordinate cations are labeled 1-7, respectively. Distances in the range 2.5-3.2 Å between H_2O groups are shown as black dashed lines and they are possible directions for hydrogen bonds.

529 Fig. 5. The crystal structures of: kazanskyite projected onto (100) (a) and nechelyustovite

530 projected onto (100) (b). Legend as in Fig. 3, Mn^{2+} dominant octahedra are pink.

531

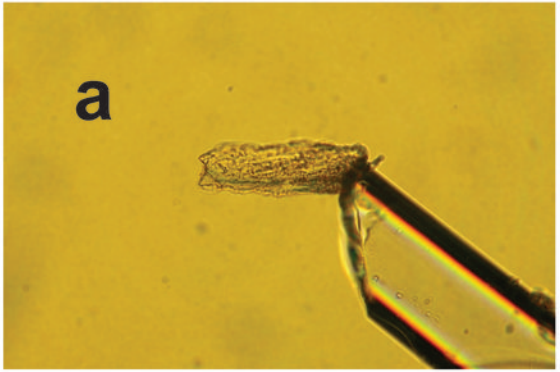
a

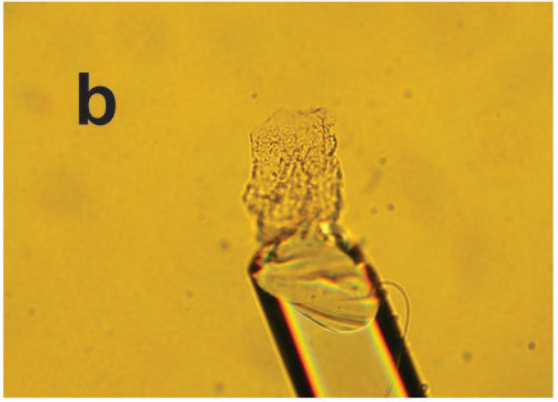
b

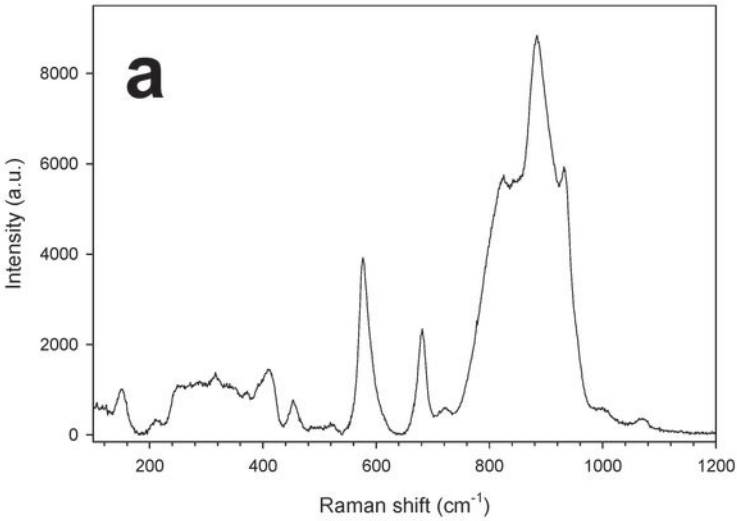
a
Intensity (a.u.)
0
2000
4000
6000
8000
200
400
600
800
1000
1200
Raman shift (cm-1)

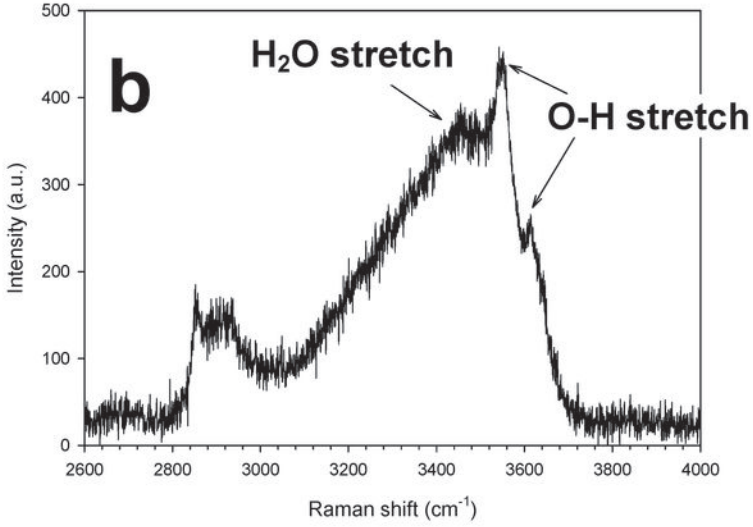
b
H2O stretch
O-H stretch
Intensity (a.u.)
0
100
200
300
400
500
2600
2800
3000
3200
3400
3600
3800
4000
Raman shift (cm-1)

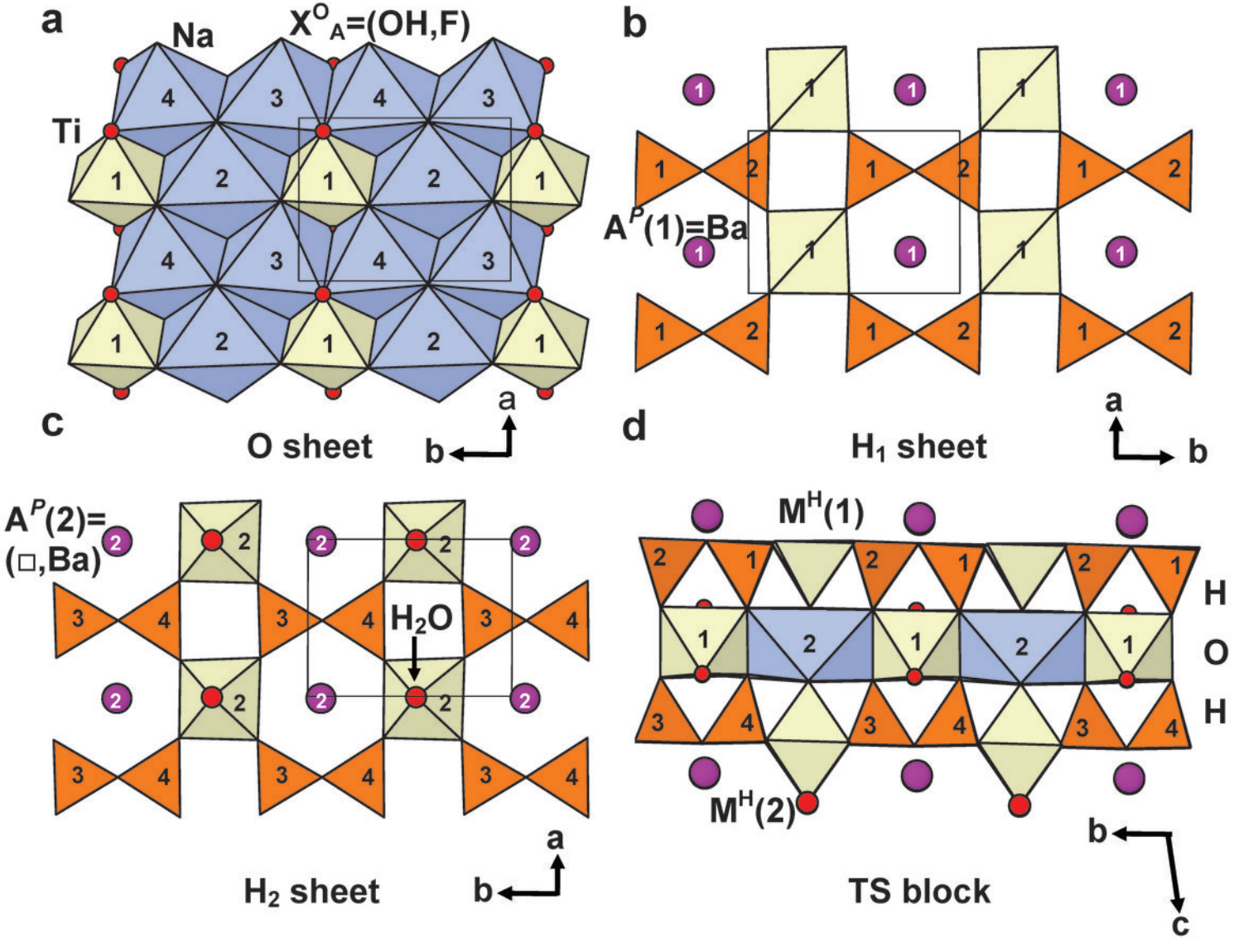
a
Na
X^{O}_{A}=(OH,F)
Ti
b
A^{P}(1)≡Ba
c
O sheet
a
b
d
H_1 sheet
a
b
A^{P}(2)=
(□,Ba)
H_2O
H_2 sheet
a
b
M^{H}(1)
H
O
H
M^{H}(2)
TS block
b
c

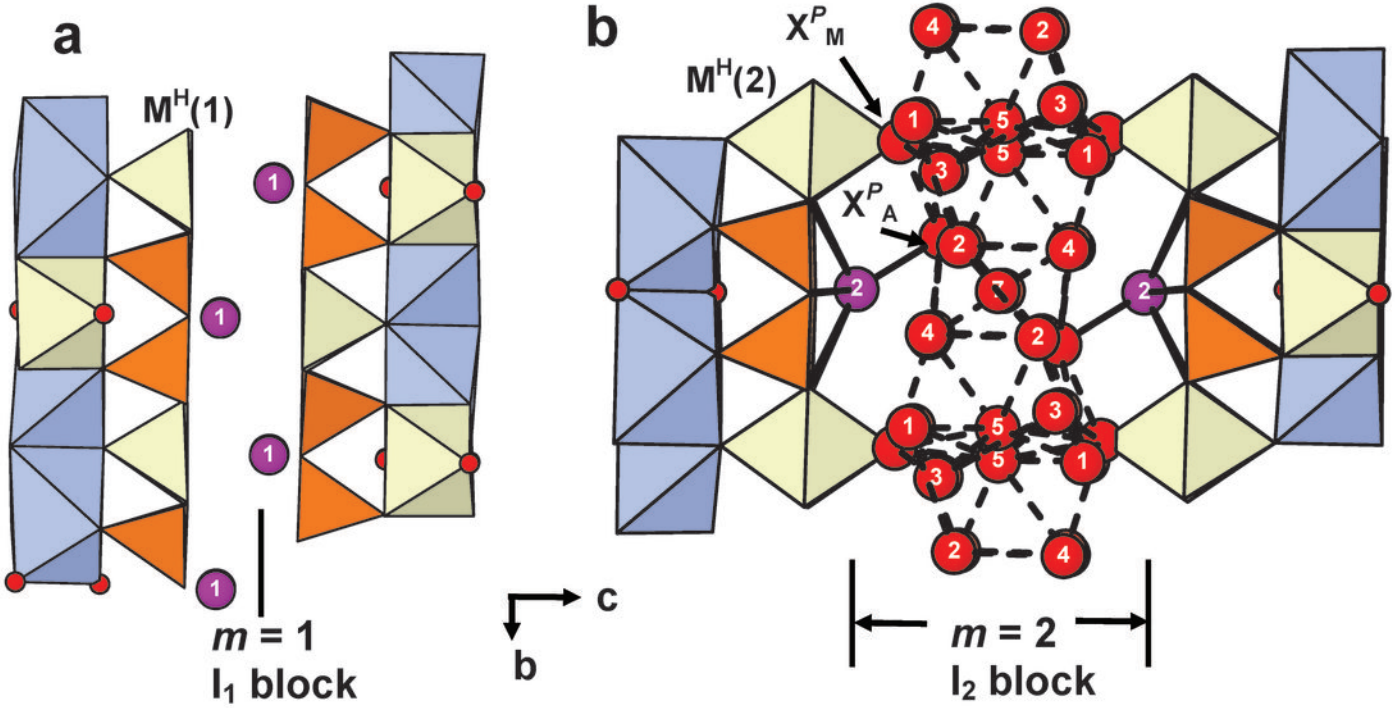
a
M^H(1)
m = 1
I1 block
b
X^P_M
M^H(2)
X^P_A
c
b
m = 2
I2 block

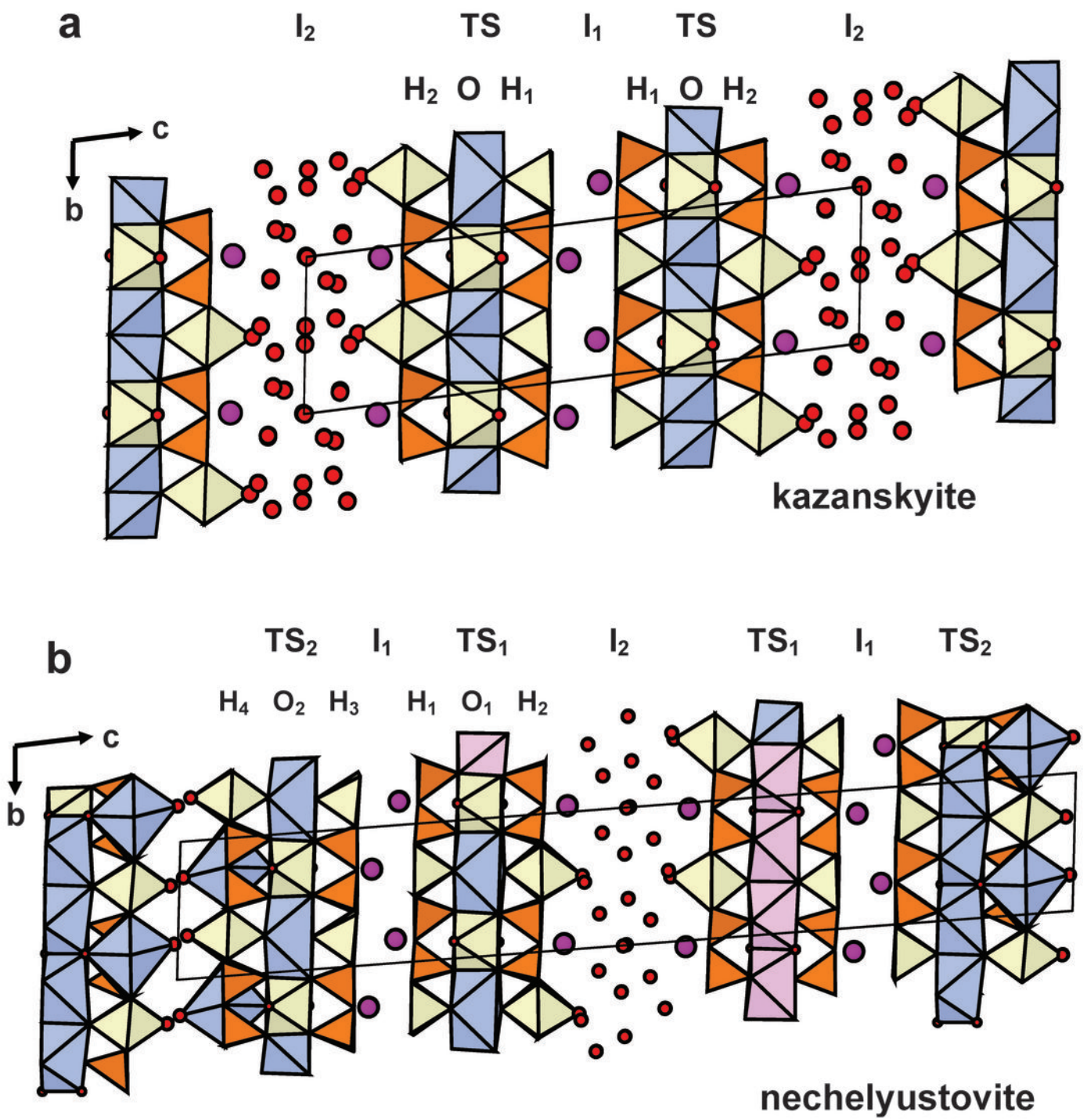
a
I2
TS
I1
TS
I2
H2 O H1
H1 O H2
c
b
kazanskyite
b
TS2
I1
TS1
I2
TS1
I1
TS2
H4 O2 H3
H1 O1 H2
c
b
nechelyustovite

Table 1. Ideal structural formulae* and unit-cell parameters for Group-III minerals with the TS block.

Mineral	Ideal structural formula								*a* (Å) α (°)	*b* (Å) β (°)	*c* (Å) γ (°)	Sp. gr.	*Z*	Ref.
	A^{P}_2	B^{P}_2	M^{H}_2	M^{O}_4	$(Si_2O_7)_2$		X^{O}_4							
lamprophyllite-2*M*	(SrNa)		**Ti_2**	**Na_3Ti**	**$(Si_2O_7)_2$**		**$O_2(OH)_2$**		19.215 90	7.061 96.797	5.3719 90	*C*2/*m*	2	(1)
lamprophyllite-2*O*	(SrNa)		**Ti_2**	**Na_3Ti**	**$(Si_2O_7)_2$**		**$O_2(OH)_2$**		19.128 90	7.0799 90	5.3824 90	*Pnmn*	2	(1)
nabalamprophyllite-2*M*	BaNa		**Ti_2**	**Na_3Ti**	**$(Si_2O_7)_2$**		**$O_2(OH)_2$**		19.741 90	7.105 96.67	5.408 90	*P*2/*m*	2	(2)
nabalamprophyllite-2*O*	(BaNa)		**Ti_2**	**Na_3Ti**	**$(Si_2O_7)_2$**		**$O_2(OH)_2$**		19.564 90	7.1173 90	5.414 90	*Pnmn*	2	(3)
barytolamprophyllite	(BaK)		**Ti_2**	**Na_3Ti**	**$(Si_2O_7)_2$**		**$O_2(OH)_2$**		19.8971 90	7.1165 96.676	5.4108 90	*C*2/*m*	2	(4)
innelite-1*T*	Ba_2	Ba_2	**Ti_2**	**$Na_2M^{2+}Ti$**	**$(Si_2O_7)_2$**	$[(SO_4)(PO_4)]$	**$O_2[O(OH)]$**		5.4234 98.442	7.131 94.579	14.785 90.009	$P\bar{1}$	1	(5)
innelite-2*M*	Ba_2	Ba_2	**Ti_2**	**$Na_2M^{2+}Ti$**	**$(Si_2O_7)_2$**	$[(SO_4)(PO_4)]$	**$O_2[O(OH)]$**		5.4206 90	7.125 94.698	29.314 90	*P*2/*c*	2	(5)
epistolite	(Na□)		**Nb_2**	**Na_3Ti**	**$(Si_2O_7)_2$**		**$O_2(OH)_2$**	$(H_2O)_4$	5.460 103.63	7.170 96.01	12.041 89.98	$P\bar{1}$	1	(6)
vuonnemite	Na_6	Na_2	**Nb_2**	**Na_3Ti**	**$(Si_2O_7)_2$**	$(PO_4)_2$	**$O_2(OF)$**		5.4984 92.60	7.161 95.30	14.450 90.60	$P\bar{1}$	1	(7)
bornemanite	Na_3	Ba	**TiNb**	**Na_3Ti**	**$(Si_2O_7)_2$**	(PO_4)	**$O_2(OH)F$**		5.4587 96.790	7.1421 96.927	24.528 90.326	$P\bar{1}$	2	(8)
kazanskyite	Ba□		**TiNb**	**Na_3Ti**	**$(Si_2O_7)_2$**		**$O_2(OH)_2$**	$(H_2O)_4$	5.4260 98.172	7.135 90.916	25.514 89.964	$P\bar{1}$	2	(9)
nechelyustovite	$Ba_2□_{1.5}Na_{0.5}$		**Ti_3 Nb**	**$(Na_{3.5}Mn_{1.5}□)Ti_2$**	**$(Si_2O_7)_4$**		**$O_4(OH)_3F$**	$(H_2O)_6$	5.4468 92.759	7.157 92.136	47.259 89.978	$P\bar{1}$	2	(10)

* For lamprophyllite, nabalamprophyllite and barytolamprophyllite, formulae are from Sokolova (2006). The invariant core of the TS block, **$M^{H}_2M^{O}_4(Si_2O_7)_2X^{O}_4$**, is shown in bold: M^{H} = cations of the H sheet; M^{O} = cations of the O sheet; X^{O}_4 = anions shared between O and H sheets; M^{2+} = Mn,Fe^{2+},Mg,Ca.

References†: (1) Krivovichev *et al.* (2003); (2) Rastsvetaeva and Chukanov (1999); (3) Sokolova and Hawthorne (2008); (4) Sokolova and Cámara (2008); (5) Sokolova *et al.* (2011); (6) Sokolova and Hawthorne (2004); (7) Ercit *et al.* (1998); (8) Cámara and Sokolova (2007); (9) this work; (10) Cámara and Sokolova (2009).

† The latest reference on the structure.

Table 2. Comparison of kazanskyite, barytolamprophyllite, nechelyustovite and bornemanite.

	kazanskyite	barytolamprophyllite	nechelyustovite			bornemanite	
Reference		(1, 4, 8)*	(7)		(3)	(6)	(2)
Formula	$Ba\square TiNbNa_3Ti(Si_2O_7)_2O_2(OH)_2(H_2O)_4$	(8): $(BaK)Na_3Ti_3(Si_2O_7)_2O_2(OH)_2$	(3): $Na_4Ba_2Mn_{1.5}\square_{2.5}Ti_5Nb(Si_2O_7)_4O_4(OH)_3F(H_2O)_6$			(2): $Na_6\square BaTi_2Nb(Si_2O_7)_2(PO_4)O_2(OH)F$	
system	triclinic	monoclinic	monoclinic	monoclinic	triclinic	orthorhombic	triclinic
space group	$P\bar{1}$	*C*2/m	*P*2/*m*	*A*2/*m*	$P\bar{1}$		$P\bar{1}$
a (Å)	5.4260(9)	10.8971	5.37	5.38	5.447	5.48	5.4587
b	7.135(1)	7.1165	7.00	7.04	7.157	7.10	7.1421
c	25.514(4)	5.4108	24.05	48.10	47.259	48.2	24.528
α (°)	98.172(4)	90	90	90	95.759		96.790
β	90.916(4)	96.676	91.1	91.1	92.136		96.927
γ	89.964(3)	90	90	90	89.978		90.326
V ($Å^3$)	977.61(3)	760.96	910	1821	1831.7	1875.4	942.4
Z	2	2	2	4	2	4	2
$D_{meas.}$ (g/cm^3)		3.543	3.32-3.42			3.47-3.50	
$D_{calc.}$ (g/cm^3)	2.930	3.521	3.20		3.041	3.20	3.342
Strongest lines in the powder pattern: d_{obs}(Å)(*I*)	2.813(100), 2.149(82), 3.938(70), 4.288(44), 2.128(44), 3.127(39), 3.690(36)	2.801(100), 2.153(90), 1.482(90), 1.601(80), 3.45(70), 1.790(70), 3.29(50)	24.06(100), 7.05(9), 5.95(97), 3.95(6), 2.828(16), 2.712(19), 2.155(13)			23.80(100), 8.02(92), 3.45(63), 2.705(24), 2.683(41), 2.410(17), 2.772(13)	
Optical character	biaxial (+)	biaxial (+)	biaxial (+)			biaxial (+)	
α	1.695	1.747	1.700			1.682	
β	1.703	1.750	1.710			1.695	
γ	1.733	1.773	1.734			1.720	
2V (°)	64.8 (meas), 55.4 (calc)	39.67 (meas)	66 (calc)			40 (meas), 66.40 (calc)	
Orientation		$Z \wedge c = 6\text{-}7^o$	*X* ~ *c*, *Y* ~ *a,* Z ~ b			*Z* = *a*, *Y* = *b,* X = c	
Color	colorless to very very pale tan	dark brown	creamy with grayish, bluish or yellowish shades			yellowish platy crystals	
Pleochroism	none observed	strong X = light-yellow, Z =brown	not discernible			weak	
Absorption		Z > Y > X	–			*Z* > *Y* = *X*	
Hardness (Mohs)	3	2-3	3			3.5 – 4	

* barytolamprophyllite: unit-cell parameters, space group and calculated density (8); powder pattern (1); D_{meas} (4); optics (1, 4); bornemanite: powder pattern (5).
References: (1) Anthony *et al*. (1995); (2) Cámara and Sokolova (2007); (3) Cámara and Sokolova (2009); (4) Dudkin (1959); (5) Ferraris *et al*., (2001); (6) Men'shikov *et al*., (1975); (7) Nèmeth *et al*., (2009); (8) Sokolova and Cámara (2008).

Table 3. Optical orientation (°) for kazanskyite.

	a	b	c
X	87.4	85.2	13.4
Y	92.1	5.1	102.8
Z	176.7	91.9	86.0

Table 4. Chemical composition and unit formula* for kazanskyite.

Oxide	wt.%	Formula unit	a.p.f.u.
Nb_2O_5	9.70	Si	4.05
TiO_2	19.41		
SiO_2	28.21	Na	2.55
Al_2O_3	0.13	Mn^{2+}	0.31
FeO	0.28	Ca	0.11
MnO	4.65	Fe^{2+}	0.03
BaO	12.50	$\Sigma 3M^{O}$	3.00
SrO	3.41		
CaO	0.89	Ti	2.09
K_2O	1.12	Nb	0.63
Na_2O	9.15	Mn^{2+}	0.26
H_2O**	9.87	Al	0.02
F	1.29	$\Sigma(2M^{H}+M^{O})$	3.00
$-O=F_2$	0.54		
Total	100.07	Ba	0.70
		Sr	0.28
		K	0.21
		Ca	0.03
		$\Sigma 2A^{P}$	1.22
		F	0.59
		OH	1.41
		ΣX^{O}_{A}	2.00
		H_2O	4.02

* calculated on anion basis: O + F = 22 a.p.f.u.;
** calculated from structure solution and refinement: OH + F = 2 a.p.f.u., H_2O = 4 a.p.f.u.

Table 5. X-ray powder diffraction data for kazanskyite*.

$I_{obs.}$	d_{obs}(Å)	d_{calc}(Å)	$I_{calc.}$	h	k	l	$I_{obs.}$	d_{obs}(Å)	d_{calc}(Å)	$I_{calc.}$	h	k	l
n.o.	n.o.	25.251	15	0	0	1		2.676	2.670		1	$\bar{1}$	$\bar{7}$
n.o.	n.o	12.626	2	0	0	2	31	2.555	2.559	25	1	$\bar{2}$	6
8	8.413	8.417	8	0	0	3		2.555	2.556		1	2	4
5	5.839	5.834	2	0	1	$\bar{3}$	82	2.149	2.155	20	2	2	$\bar{2}$
9	5.324	5.322	1	1	0	$\bar{1}$		2.149	2.153	36	2	$\bar{2}$	0
8	5.035	5.050	1	0	0	5		2.149	2.151		2	0	7
10	4.599	4.594	2	1	0	$\bar{3}$		2.149	2.150		2	2	0
44	4.288	4.300	11	1	1	$\bar{1}$		2.149	2.149		2	$\bar{2}$	2
	4.288	4.306		1	$\bar{1}$	0	44	2.128	2.134	23	2	2	$\bar{3}$
	4.288	4.299		1	1	0		2.128	2.132		2	$\bar{2}$	$\bar{1}$
	4.288	4.298		1	$\bar{1}$	1		2.128	2.127		1	$\bar{3}$	4
70	3.938	3.954	17	1	$\bar{1}$	3		2.128	2.124		2	2	1
	3.938	3.952		1	1	2		2.128	2.124		2	$\bar{2}$	3
30	3.714	3.723	12	1	$\bar{1}$	$\bar{3}$	26	2.043	2.050	19	2	$\bar{2}$	$\bar{3}$
36	3.690	3.686	10	1	$\bar{1}$	4		2.043	2.050		1	$\bar{2}$	$\bar{8}$
20	3.432	3.447	15	1	1	$\bar{5}$	22	2.034	2.035	21	2	2	3
	3.432	3.441		1	$\bar{1}$	$\bar{4}$		2.034	2.036		2	$\bar{2}$	5
39	3.127	3.128	24	1	$\bar{1}$	6		2.034	2.031		0	3	$\bar{8}$
	3.127	3.124		1	1	5	17	2.013	2.012	18	2	$\bar{1}$	8
32	2.955	2.962	14	1	$\bar{2}$	0		2.013	2.011		2	1	7
	2.955	2.957		1	2	0	11	1.916	1.915	12	2	$\bar{1}$	9
	2.955	2.957		1	$\bar{2}$	2		1.916	1.914		2	1	8
33	2.895	2.896	36	1	$\bar{2}$	3	19	1.760	1.765	18	2	3	$\bar{4}$
	2.895	2.895		1	2	1		1.760	1.763		2	$\bar{3}$	$\bar{1}$
100	2.813	2.820	100	1	2	$\bar{4}$		1.760	1.759		2	1	$\bar{1}\bar{1}$
	2.813	2.815		1	$\bar{2}$	$\bar{2}$		1.760	1.759		2	$\bar{3}$	4
19	2.707	2.702	20	2	0	$\bar{1}$		1.760	1.758		2	3	1
20	2.696	2.693	40	2	0	1		1.760	1.757		2	$\bar{1}$	$\bar{1}0$
23	2.685	2.688	21	1	$\bar{2}$	5	26	1.608	1.611	54	3	$\bar{2}$	0
	2.685	2.685		1	2	3		1.608	1.609		3	2	0
20	2.676	2.674	21	1	1	$\bar{8}$		1.608	1.608		3	$\bar{2}$	2

* Indexed on a = 5.426(3), b = 7.122(5), c = 25.53(2) Å, α = 98.24(6), β = 90.82(5), γ = 89.93(3)°, V = 976.3(8)Å3; d_{calc}, I_{calc}, and *hkl* values are from the powder pattern calculated from single-crystal data. n.o.: not observed (covered by beamstop)

Table 6. Miscellaneous refinement data for kazanskyite.

a (Å)	5.4260(9)
b	7.135(1)
c	25.514(4)
α (°)	98.172(4)
β	90.916(4)
γ	89.964(3)
V (Å^3)	977.61(3)
Space group	$P\bar{1}$
Z	2
Absorption coefficient (mm^{-1})	4.20
F(000)	829.2
$D_{calc.}$ (g/cm^3)	2.930
Crystal size (mm)	0.01 x 0.05 x 0.15
Radiation/filter	MoKα/graphite
2θ-range for data collection (°)	3.22 - 50.05
R(int) (%)	5.25
Reflections collected	13481
Independent reflections $F_o > 4\sigma F$	3471 3066
Refinement method	Full-matrix least squares on F^2, fixed weights proportional to $1/\sigma F_o^2$
No. of refined parameters	224
Final $R_{(obs)}$ (%) [$F_o > 4\sigma F$]	8.09
R_1	9.47
wR_2	20.51
Highest peak, deepest hole (e Å^{-3})	+1.841 -1.705
Goodness of fit on F^2	1.090

Table 7. Atom coordinates and isotropic temperature parameters for kazanskyite.

Atom	Site occupancy	*x*	*y*	*z*	U_{iso} (Å^2)*
M^O(1)	1	0.3962(4)	0.1432(4)	0.30847(8)	0.0275(7)
M^O(2)	1	0.3811(8)	0.6373(11)	0.30400(17)	0.0325(10)
M^O(3)	1	0.8873(10)	0.8954(5)	0.3032(2)	0.0126(10)
M^O(4)	1	0.8860(9)	0.3828(5)	0.3042(2)	0.0115(9)
M^H(1)	1	0.7444(3)	0.7059(5)	0.41946(13)	0.0143(4)
M^H(2)	1	0.0172(2)	0.5759(3)	0.18391(5)	0.0174(4)
Si(1)	1	0.2464(8)	0.4164(5)	0.41368(16)	0.0111(8)
Si(2)	1	0.2425(8)	-0.0159(5)	0.41606(17)	0.0114(9)
Si(3)	1	0.5125(8)	0.8740(5)	0.19727(17)	0.0112(9)
Si(4)	1	0.5249(9)	0.2961(6)	0.1986(2)	0.0270(12)
A^P(1)	0.96	0.74633(11)	0.23498(17)	0.47349(3)	0.0109(2)
A^P(2)	0.26	0.0134(6)	0.0654(11)	0.13298(17)	0.0337(9)
O(1)	1	0.509(2)	0.9151(15)	0.2592(4)	0.022(3)
O(2)	1	0.5172(14)	0.0709(7)	0.1730(3)	0.0311(18)
O(3)	1	0.772(2)	0.3756(19)	0.1770(6)	0.048(4)
O(4)	1	0.4822(15)	0.5378(13)	0.4403(5)	0.020(3)
O(5)	1	0.2463(10)	0.2149(7)	0.4407(2)	0.0140(13)
O(6)	1	0.4966(17)	0.9104(13)	0.4390(4)	0.009(2)
O(7)	1	-0.001(2)	0.9026(14)	0.4423(5)	0.017(2)
O(8)	1	0.237(2)	0.3665(14)	0.3515(3)	0.021(3)
O(9)	1	0.003(2)	0.5246(13)	0.4364(4)	0.012(2)
O(10)	1	0.237(2)	0.9584(14)	0.3520(4)	0.015(2)
O(11)	1	0.2794(13)	0.7562(12)	0.1739(4)	0.023(2)
O(12)	1	0.538(2)	0.3295(15)	0.2645(4)	0.022(3)
O(13)	1	0.2660(19)	0.3712(15)	0.1753(4)	0.032(3)
O(14)	1	0.7545(18)	0.7683(14)	0.1752(4)	0.023(3)
X^O_M(1) O	1	0.7441(12)	0.6633(18)	0.3537(3)	0.0202(16)
X^O_M(2) O	1	0.0241(14)	0.6106(19)	0.2562(3)	0.033(2)
X^O_A(1) OH,F	1	0.6785(12)	0.1640(19)	0.3521(3)	0.0216(16)
X^O_A(2) OH,F	1	0.0814(12)	0.1146(16)	0.2642(3)	0.0213(17)
X^P_M H_2O	1	0.0061(17)	0.531(3)	0.0952(4)	0.050(3)
X^P_A H_2O	0.26	0.235(8)	0.199(6)	0.0563(18)	0.05
W(1)** H_2O	0.71	0.507(3)	0.593(2)	0.0809(6)	0.05
W(2) H_2O	0.46	0.511(5)	0.167(4)	0.0370(10)	0.05
W(3) H_2O	0.34	0.523(6)	0.416(5)	0.0546(14)	0.05
W(4) H_2O	0.29	0.502(8)	0.892(6)	0.0644(16)	0.05
W(5) H_2O	0.25	0.145(8)	0.446(6)	0.0001(16)	0.05
W(6) H_2O	0.40	-0.013(6)	0.880(4)	0.0644(12)	0.05
W(7) H_2O	0.31	0.298(5)	-0.002(9)	-0.0011(11)	0.05

Table 7. continued

Atom	Site occupancy	*x*	*y*	*z*	U_{iso} (Å^2)*
Subsidiary peaks**					
A^P(1A)	0.02	0.734(7)	0.203(10)	0.4236(14)	0.02
A^P(1B)	0.02	0.247(7)	0.743(11)	0.4903(19)	0.02
A^P(2A)	0.07	0.0138(18)	0.0517(16)	0.1654(5)	0.02
A^P(2B)	0.03	0.990(4)	0.110(3)	0.0956(10)	0.02
M^H(1A)	0.03	0.758(5)	0.728(8)	0.4486(16)	0.02
M^H(1B)	0.03	0.750(5)	0.676(7)	0.3923(19)	0.02
1	0.04	0.212(3)	0.443(3)	0.0587(7)	0.02
2	0.04	0.797(3)	0.436(2)	0.0581(7)	0.02
3	0.02	0.980(8)	0.636(6)	0.0519(18)	0.02

* U_{eq} for M^O(1,3,4), M^H(2), Si(4), A^P(1,2);
** for W(1-7) and subsidiary peaks, U_{iso} = 0.05 and 0.02 (fixed), respectively.

Table 8. Selected interatomic distances (Å) and angles (°) for kazanskyite.

$M^{O}(1)$-$X^{O}_{A}(1)$	1.873(7)	$M^{O}(2)$-$X^{O}_{M}(2)$	2.266(9)	$M^{O}(3)$-$X^{O}_{A}(2)$b	2.24(1)
$M^{O}(1)$-O(8)	2.01(1)	$M^{O}(2)$-$X^{O}_{M}(1)$	2.319(8)	$M^{O}(3)$-O(10)c	2.26(1)
$M^{O}(1)$-O(1)a	2.01(1)	$M^{O}(2)$-O(12)	2.44(1)	$M^{O}(3)$-$X^{O}_{M}(2)$c	2.34(1)
$M^{O}(1)$-O(12)	2.02(1)	$M^{O}(2)$-O(1)	2.53(1)	$M^{O}(3)$-O(1)	2.34(1)
$M^{O}(1)$-$X^{O}_{A}(2)$	2.027(7)	$M^{O}(2)$-O(8)	2.55(1)	$M^{O}(3)$-$X^{O}_{M}(1)$	2.38(1)
$M^{O}(1)$-O(10)	2.04(1)	$M^{O}(2)$-O(10)	2.51(1)	$M^{O}(3)$-$X^{O}_{A}(1)$d	2.42(1)
$<M^{O}(1)$-φ>	2.00	$<M^{O}(2)$-O>	2.45	$<M^{O}(3)$-φ>	2.33
$M^{O}(4)$-O(12)	2.14(1)	Si(1)-O(8)	1.576(8)	Si(2)-O(6)a	1.606(8)
$M^{O}(4)$-O(8)c	2.25(1)	Si(1)-O(9)	1.60(1)	Si(2)-O(10)a	1.62(1)
$M^{O}(4)$-$X^{O}_{A}(2)$c	2.30(1)	Si(1)-O(4)	1.630(1)	Si(2)-O(7)a	1.64(1)
$M^{O}(4)$-$X^{O}_{M}(2)$c	2.30(1)	Si(1)-O(5)	1.680(1)	Si(2)-O(5)	1.678(5)
$M^{O}(4)$-$X^{O}_{M}(1)$	2.35(1)	<Si(1)-O>	1.62	<Si(2)-O>	1.64
$M^{O}(4)$-$X^{O}_{A}(1)$	2.41(1)				
$<M^{O}(1)$-φ>	2.29	Si(3)-O(1)	1.57(1)	Si(4)-O(3)	1.593(9)
		Si(3)-O(11)	1.580(1)	Si(4)-O(13)	1.64(1)
Si(3)a-O(2)-Si(4)	134.5(4)	Si(3)-O(14)	1.59(1)	Si(4)-O(2)	1.647(6)
Si(1)-O(5)-Si(2)	134.2(4)	Si(3)-O(2)d	1.615(1)	Si(4)-O(12)	1.66(1)
<Si-O-Si>	134.4	<Si(3)-O>	1.59	<Si(4)-O>	1.64
$M^{H}(1)$-$X^{O}_{M}(1)$	1.667(1)	$M^{H}(2)$-$X^{O}_{M}(1)$	1.824(8)		
$M^{H}(1)$-O(4)	1.988(9)	$M^{H}(2)$-O(3)e	1.94(1)		
$M^{H}(1)$-O(7)c	1.99(1)	$M^{H}(2)$-O(11)	1.963(7)		
$M^{H}(1)$-O(9)c	1.99(1)	$M^{H}(2)$-O(13)	1.98(1)		
$M^{H}(1)$-O(6)	2.000(9)	$M^{H}(2)$-O(14)e	2.01(1)		
$<M^{H}(1)$-O>	1.93	$M^{H}(2)$-X^{P}_{M}	2.240(9)		
		$<M^{H}(2)$-φ>	1.99		
$A^{P}(1)$-O(6)a	2.71(1)	$A^{P}(2)$-X^{P}_{A}	2.61(5)		
$A^{P}(1)$-O(7)	2.76(1)	$A^{P}(2)$-O(13)	2.66(1)		
$A^{P}(1)$-O(9)c	2.78(1)	$A^{P}(2)$-O(3)e	2.69(2)		
$A^{P}(1)$-O(4)	2.81(1)	$A^{P}(2)$-O(14)g	2.89(1)		
$A^{P}(1)$-O(5)	2.824(6)	$A^{P}(2)$-O(2)e	2.893(8)		
$A^{P}(1)$-O(7)f	2.83(1)	$A^{P}(2)$-O(2)	2.900(8)		
$A^{P}(1)$-O(4)f	2.84(1)	$A^{P}(2)$-O(11)a	2.94(1)		
$A^{P}(1)$-O(5)c	2.849(6)	$<A^{P}(2)$-φ>	2.80		
$A^{P}(1)$-O(6)f	2.92(1)				
$A^{P}(1)$-O(9)f	2.97(1)				
$<A^{P}(1)$-O>	2.83				

φ = unspecified anion; a: *x*, *y*-1, *z*; b: *x*+1, *y*+1, *z*; c: *x*+1, *y*, *z*; d: *x*, *y*+1, *z*; e: *x*-1, *y*, *z*; f: -*x*+1, -*y*+1, -*z*+1; g: *x*-1, *y*-1, *z*; h: *x*+1, *y*-1, *z*.

Table 9. Refined site-scattering and assigned site-populations for kazanskyite.

Site	Refined site-scattering (e.p.f.u.)	Assigned site-population (a.p.f.u.)	Calculated site-scattering (e.p.f.u.)	$\langle X\text{-}\varphi\rangle_{calc.}$* (Å)	$\langle X\text{-}\varphi\rangle_{obs.}$ (Å)
$M^{O}(1)$**	21.6(2)	0.74 Ti + 0.26 Mn	22.8	2.03	2.00
$M^{O}(2)$	11.0	1.0 Na	11.0	2.40	2.45
$M^{O}(3)$	14.0***	0.78 Na + 0.11 Ca + 0.11 Mn	13.5	2.37	2.33
$M^{O}(4)$	14.0***	0.77Na + 0.20 Mn+ 0.03 Fe^{2+}	14.3	2.34	2.29
$^{[5]}M^{H}(1)$	21.7(2)	0.98 Ti + 0.02 Al	21.8	1.89	1.93
$M^{H}(2)$	32.2(2)	0.63 Nb + 0.37 Ti	34.0	2.00	1.99
$^{[10]}A^{P}(1)$	42.9***	0.56 Ba + 0.22 Sr + 0.15 K + 0.03 Ca + 0.04 □	43.2		2.83
$^{[7]}A^{P}(2)$	11.2***	0.74 □ + 0.14 Ba + 0.06 Sr + 0.06 K	11.3		2.80

X = cation, φ = O, OH, F, H_2O;
* calculated by summing constituent ionic radii; values from Shannon (1976),
** coordination number is given only for non-[6]-coordinated sites;
*** site scattering was refined, adjusted in accord with chemical analysis (Table 4), and then fixed at the last stages of the refinement (see discussion in text).

Table 10. Bond valences (v.u.) for kazanskyite.

Atom	Si(1)	Si(2)	Si(3)	Si(4)	$M^{O}(1)$	$M^{O}(2)$	$M^{O}(3)$	$M^{O}(4)$	$M^{H}(1)$	$M^{H}(2)$	$A^{P}(1)$	$A^{P}(2)$	Σ
O(1)			1.15		0.56	0.16	0.24						2.11
O(2)			1.02	0.94								0.04, 0.04	2.04
$^{[3]}$O(3)				1.08						0.83		0.07	1.98
O(4)	0.98								0.60		0.20, 0.18		1.96
O(5)	0.86	0.86									0.19, 0.18		2.09
O(6)		1.04							0.58		0.25, 0.15		2.02
O(7)		0.95							0.60		0.22, 0.19		1.96
O(8)	1.13				0.56	0.16		0.27					2.12
O(9)	1.06								0.60		0.21, 0.13		2.00
O(10)		1.01			0.52	0.15	0.28						1.96
$^{[3]}$O(11)			1.12							0.79		0.04	1.95
O(12)				0.91	0.55	0.19		0.35					2.00
$^{[3]}$O(13)				0.95						0.75		0.08	1.78
$^{[3]}$O(14)			1.09							0.70		0.04	1.83
$X^{O}_{M}(1)$						0.24	0.22	0.23	1.50				2.19
$X^{O}_{M}(2)$						0.26	0.24	0.25		1.11			1.86
$^{[3]}X^{O}_{A}(1)$					0.82		0.21	0.20					1.23
$^{[3]}X^{O}_{A}(2)$					0.54		0.29	0.25					1.08
$^{[1]}X^{P}_{M}$										0.40			0.40
$^{[1]}X^{P}_{A}$												0.09	0.09
Total	4.03	3.86	4.38	3.88	3.55	1.16	1.48	1.55	3.88	4.58	1.90	0.40	
Aggregate charge	4.00	4.00	4.00	4.00	3.48	1.00	1.22	1.23	3.98	4.63	1.77	0.46	

* bond-valence parameters are from Brown (1981); coordination numbers are shown for non-[4]-coordinated anions; $X^{O}_{A}(1,2)$: monovalent anions, mainly OH, less F (see Table 7); X^{P}_{M} and X^{P}_{A}: H_2O groups; X^{P}_{A} is 26% occupied by H_2O.

Table 11. The O–O distances* (Å) for H_2O groups in the $\mathbf{I}_2$ block.

	X^P_M	X^P_A	W(1)	W(2)	W(3)	W(4)	W(5)	W(6)	W(7)
X^P_M		2.74(5)	2.79(2)		3.08(4)		2.54(4)	2.71(3)	
X^P_M a			2.77(2)		2.88(4)				
X^P_M b							2.58(4)		
X^P_A	2.74(5)		3.15(5)	[1.59(5)]			[2.47(6)]		[1.93(7)]
X^P_A c						2.66(6)		2.68(5)	
X^P_A d									3.15(6)
W(1)	2.79(2)	3.15(5)		3.09(3)	[1.35(4)]	[2.23(4)]	2.91(4)		
W(1)e	2.77(2)								
W(1)f							2.80(4)		
W(2)		[1.59(5)]	3.09(3)		[1.77(4)]		3.04(5)		[1.83(5)]
W(2)d				2.83(5)					[1.74(5)]
W(2)c						[2.18(4)]			
W(2)f						2.56(5)			
W(3)	3.08(4)	[2.20(6)]	[1.35(4)]	[1.77(4)]			[2.49(5)]		
W(3)e	2.88(4)								
W(3)f							2.58(5)		
W(4)			[2.23(4)]					2.79(5)	
W(4)g		2.66(6)		[2.18(4)]					[2.21(6)]
W(4)f				2.56(5)					[2.20(6)]
W(4)e								2.64(5)	
W(5)	2.54(4)	[2.47(6)]	2.91(4)	3.04(5)	2.49(5)				
W(5)b	2.58(4)						[1.75(8)]	2.74(5)	
W(5)f			2.80(4)		2.58(5)				
W(6)	2.71(3)					2.79(5)			
W(6)g		2.68(5)							2.62(5)
W(6)a						2.64(5)			
W(6)b							2.74(5)		[2.47(5)]
W(7)		[1.93(7)]		[1.83(5)]					
W(7)d		3.15(6)		[1.74(5)]					[2.19(6)]
W(7)f						[2.20(6)]			
W(7)c						[2.21(6)]		2.62(5)	
W(7)b								[2.47(5)]	

a: *x*+1, *y*, *z*; b: -*x*, -*y*+1, -*z*; c: *x*, *y*+1, *z*; d: -*x*+1, -*y*, -*z*; e: *x*-1, *y*, *z*; f: -*x*+1, -*y*+1, -*z*; g: *x*, *y*-1, *z*;

* O-O distances < 2.50 Å are given in [ ].